

## Chapter

# Bragg Grating Tuning Techniques for Interferometry Applications

*Rogério Dionísio*

## Abstract

Fiber Bragg grating is widely used in optical fiber applications as a filter or a sensor due to its compact size and high sensitivity to physical conditions, such as temperature and strain. The purpose of this chapter is to describe the implementation and characterization of two tuning methods for optical fiber Bragg gratings, varying the temperature or the length of the fiber. Among the methods using mechanical deformation, compression of the fiber by bending a flexible sheet aggregated with the Bragg grating has shown very interesting tuning results, reaching 19.0 nm with minimum reflection bandwidth variation over the entire tuning range. Stretching the fiber has presented several drawbacks, including breaking of the fiber and a lower tuning range of 4.9 nm. Temperature tuning technique presents good linearity between tuning range and temperature variation but at the cost of a low tuning range (0.4 nm) and a permanent high current electrical source.

**Keywords:** fiber Bragg grating, tuning system, thermal tuning, mechanical tuning, experimental characterization

## 1. Introduction

Fiber optic Bragg gratings (FBGs) were first produced in 1978 by Ken Hill et al., during an experiment where an optical fiber was exposed to intense radiation from an argon laser. The interference process started between the incident wave and the 4% light reflected at the opposite end of the fiber [1]. It was not until a decade later, in 1989, that G. Meltz and his team proposed Bragg gratings production process by exposing the fiber transversely to two coherent beams of ultraviolet light, forming an interference pattern in the fiber core [2, 3].

Over the last decades, Bragg gratings have been used as sensors [4, 5] or as optical filters in wavelength division multiplexing (WDM) communication systems [6]. They have found application in devices with routing capacity in the optical domain, as is the case of optical add drop multiplexers (OADM) and optical cross connect (OXC) nodes. They are also used in frequency stabilizers of semiconductor lasers [7], on tunable fiber lasers [8], and in the gain equalization of optical amplifiers [9]. Fiber dispersion compensation [10] is another realization with tunable fiber Bragg gratings.

The evolution of transmission systems from point-to-point connections to dynamically configurable networks brought the need for tunable optical filters. Furthermore,

the increasing transfer of information over fiber optic networks causes an increase in the number of optical channels in Dense (DWDM) or even in Coarse WDM (CWDM). The expansion in the bandwidth necessity range can cover the S, C, L, and U bands, corresponding approximately to 215 nm.

During the last 3 decades, but also very recently, the use of spread spectrum techniques in the optical domain, such as optical code division multiplexing (OCDMA), has stirred the interest of the scientific community, as an option in reconfigurable optical networks [11]. This process allows the various channels to share the same spectral band; each one being identified by a specific code. Other features of this technique should be highlighted: Greater safety in the data transmission, more flexible use of available bandwidth, reducing crosstalk between adjacent channels, and enabling asynchronous communication [12]. The recent use of spectral amplitude coding OCDMA (SAC-OCDMA) in optical coding and decoding systems has brought the ability to eliminate multiple access interference (MAI) [13]. For this technique to be attractive from the point of view of implementation in an optical network, the definition of the codes will have to be flexible [14], so that tunable FBGs are a key element of the process. One of the features that make FBGs attractive is that the reflection spectrum can be tuned from a few nanometers, heating the Bragg grating or applying mechanical tension to the ends (compression or extension).

The objective of this chapter is to describe the implementation of two tuning methods for fiber Bragg gratings, as a function of variations in temperature or in the length of the FBG. Among the methods of mechanical deformation, the deformation of the grating by stretching or compressing the fiber and the deformation by curvature of a flexible blade connected to the Bragg grating are experimentally implemented and discussed.

The rest of the chapter is structured as follows: Section 2 presents the operating principle of FBG tuning techniques using mechanical and temperature techniques. Section 3 describes the experimental measurement setup for FBG tuning characterization. Section 4 presents the main experimental results and discusses the potential of each tuning technique. Finally, Section 5 gives concluding remarks.

## 2. Operating principle

The resonant wavelength ( $\lambda_B$ ) of a Bragg grating depends on the effective refractive index at the fiber core ( $n_{eff}$ ) and the period of the interference pattern ( $\Lambda$ ) [15],

$$\lambda_B = 2 \cdot n_{eff} \cdot \Lambda \quad (1)$$

In turn, these parameters are affected by temperature variations or mechanical deformations. From **Eq. (1)**, the deviation of the Bragg wavelength due to mechanical deformations  $\Delta l$ , or temperature variations  $\Delta T$  [16] are:

$$\Delta \lambda_B = 2 \left( \Lambda \frac{\delta n_{eff}}{\delta l} + n_{eff} \frac{\delta \Lambda}{\delta l} \right) \Delta l + 2 \left( \Lambda \frac{\delta n_{eff}}{\delta T} + n_{eff} \frac{\delta \Lambda}{\delta T} \right) \Delta T \quad (2)$$

The first term of **Eq. (2)** represents the dependence of  $\lambda_B$  as a function of  $\Delta l$ , caused by variations in the grating period and the change in the effective refractive index. This term can be described by:

$$\Delta\lambda_B = (1 - \rho_e) \cdot \varepsilon_{rel} \cdot \lambda_B, \quad (3)$$

where  $\varepsilon_{rel}$  is the relative elongation and  $\rho_e$  is the effective elasto-optic coefficient. For a silica optical fiber,  $\rho_e \approx 0.22$  [17].

The second term of expression (2) represents the effect of temperature on changing the Bragg wavelength. For a Bragg grating with maximum reflectivity at 1550 nm, the typical values of sensitivity to temperature and mechanical stress are, respectively, 13.25 pm/°C and 1.2 pm/ $\mu\varepsilon$  [16].

It is therefore predictable that any change in wavelength associated with external disturbances is the result of the sum of the effects of temperature and mechanical deformations. Therefore, the individual discrimination in the spectral response of the FBG for each source of disturbance needs a method of separating the measurements. Briefly, the existing methods are extrinsic or intrinsic and are reported in detail in [16]. In Section 4.1, a set of tuning experiments is described, based on stretching or compressing the fiber, and which take place in a laboratory in a controlled temperature environment. Under these conditions, the influence of temperature on the wavelength variation is very small compared to the variations induced by the mechanical compression or stretching methods.

## 2.1 Mechanical linear tuning

**Figure 1** illustrates the elements that make up a tuning system by mechanical tension on the fiber. The ends of the optical fiber are fixed on two supports, where at least one must be able to move along the axial axis of the fiber.

The relative elongation along the axial axis is defined by

$$\varepsilon_{rel} = \frac{\Delta z}{L}, L \neq 0, \quad (4)$$

where  $\Delta z$  is the displacement and  $L$  is the length of the fiber under the effect of a mechanical deformation [18]. Substituting this result into **Eq. (3)**, we get:

$$\Delta\lambda_B = (1 - \rho_e) \cdot \frac{\Delta z}{L} \cdot \lambda_B, L \neq 0 \quad (5)$$

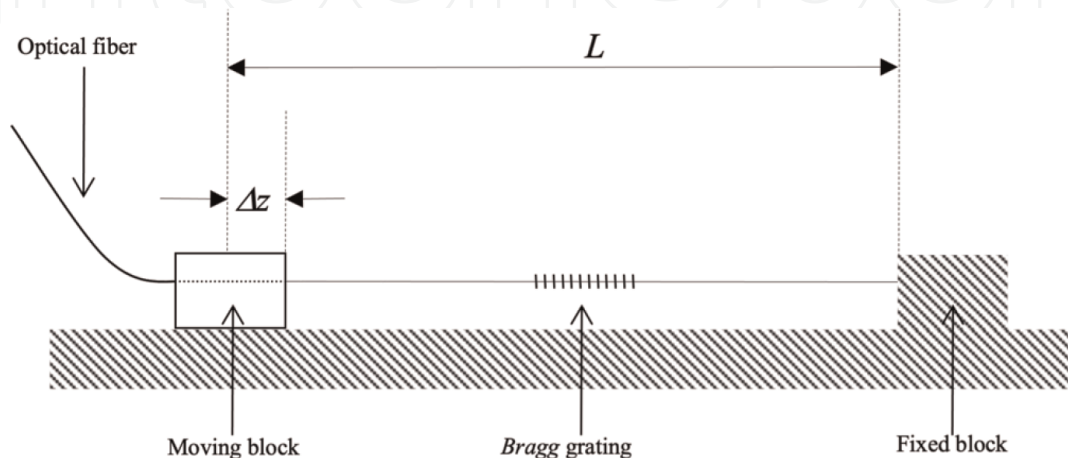


**Figure 1.** Schematic of the structure of a tuning system for fiber optic Bragg networks.

The result is an equation that relates the variation of the Bragg wavelength as a function of the normalized fiber length. The change in wavelength will be positive or negative if the Bragg grating undergoes stretching or compression, respectively. Considering that the displacement is much smaller than the length of the grating, Eq. (5) is approximately linear.

## 2.2 Mechanical tuning by bending

Figure 2 shows the scheme of a tuning system, in which a force is applied to a flexible blade. Horizontal displacement  $\Delta z$  causes the blade to bend in an arc with angle  $\theta$ . The relationship between the angle arc  $\theta$  and the displacement  $\Delta z$  is given by:

$$\Delta z = L \left[ 1 - \frac{\sin\left(\frac{\theta}{2}\right)}{\left(\frac{\theta}{2}\right)} \right], \quad (6)$$

where  $L$  is the length of the blade in the initial state, with no force applied to it [19, 20].

For an optical fiber embedded in an elastic material at a distance  $d$  from the blade, the relative elongation is given by [19–21]:

$$\varepsilon_{rel} = \mp \frac{d \cdot \theta}{L}, L \neq 0 \quad (7)$$

The negative sign corresponds to a compressive force when the blade is bent upwards, while a positive sign in the second term of Eq. (7) indicates a pulling force on the fiber, bending the blade downwards.

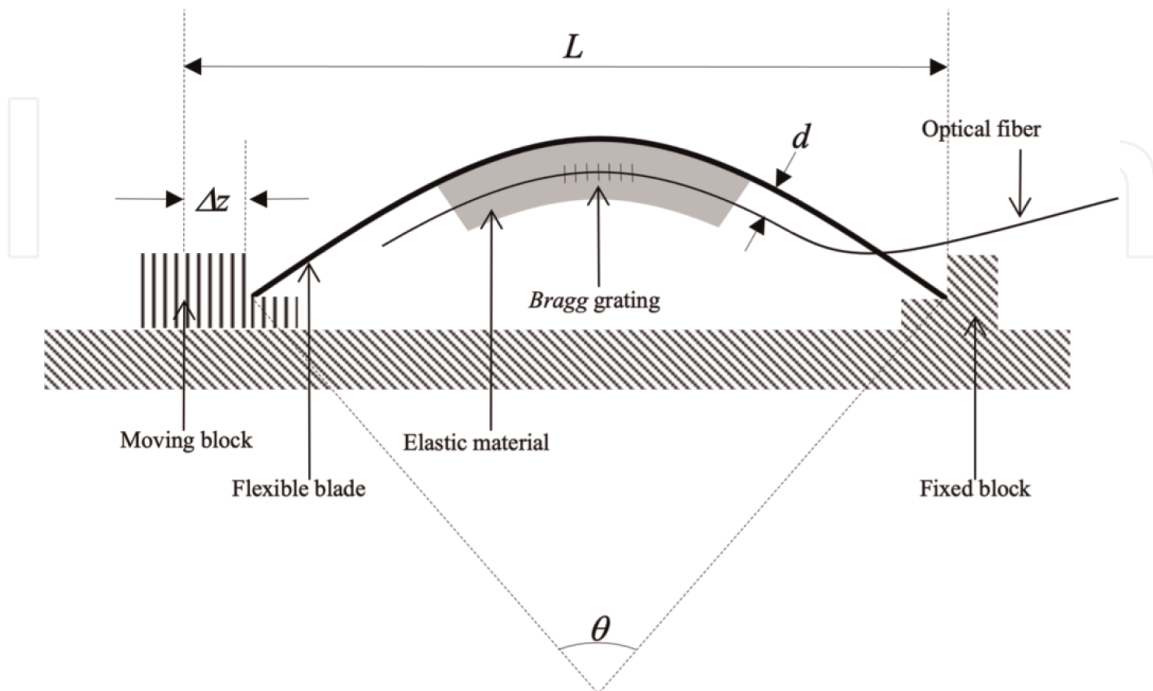


Figure 2. Schematic of the structure of a tuning system based on bending a flexible blade.

Conjugating (3), (6), and (7) into a single equation,

$$\frac{\Delta z}{L} = 1 - \text{sinc}\left(\frac{\Delta\lambda_B \cdot L}{2 \cdot \pi \cdot d \cdot (1 - \rho_e) \cdot \lambda_B}\right), L \neq 0 \quad (8)$$

The relationship between the spectral tuning  $\lambda_B$  and the displacement is not linear, contrary to the result in the procedure in Section 4.1.

### 2.3 Temperature tuning

The second term of Eq. (2) provides an explicit relationship of the dependence of the Bragg wavelength on temperature variations and is expressed by:

$$\Delta\lambda_B = (\alpha_T + \xi_T) \cdot \Delta T \cdot \lambda_B, \quad (9)$$

where  $\alpha_T$  is the thermal expansion coefficient and  $\xi_T$  is the thermo-optical coefficient. In the case of silica, the mentioned constants have the following values:  $\alpha_T = 0.55 \times 10^{-6} K^{-1}$  and  $\xi_T = 8.0 \times 10^{-6} K^{-1}$ .

A possible tuning scheme is to place the Bragg grating over a thermoelectric module, also called a Peltier cell, and envelop the set-in thermal mass. The objective is to standardize the temperature in the network and increase the thermal conductivity between the optical fiber and the Peltier module [22, 23].

It is also possible to increase the thermal sensitivity of the optical fiber by fixing it on a metallic surface. If a zinc (Zn) sheet is used, it is possible to increase the sensitivity to 40.8 pm/K. By fixing two Peltier modules at the ends of the zinc sheet, a temperature gradient is created that causes a linear variation of the grating period, which is used to tune the Bragg wavelength, maintaining a constant group delay. For this, the temperature difference between the two ends is kept constant, while the temperature at both ends is increased or decreased by the same amount [24].

### 3. Laboratory measurement system

To characterize the tuning methods, an optical measurement system was set up, whose implementation scheme is shown in Figure 3. It is based on the measurement of the spectral component reflected by the network when illuminated by an optical

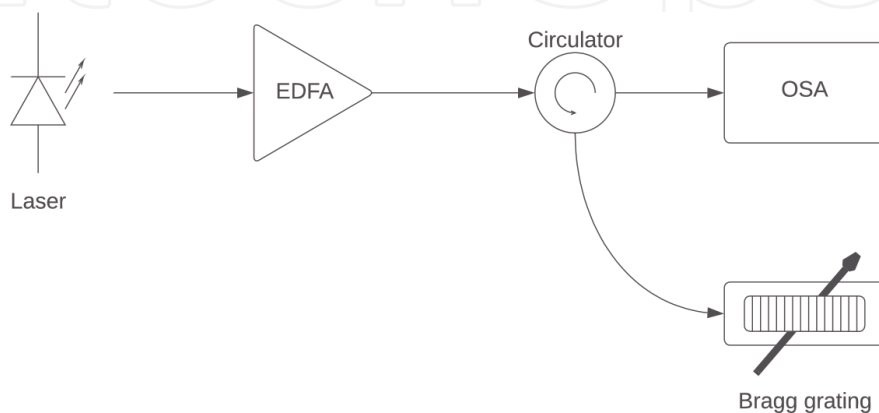


**Figure 3.** Experimental setup used to determine the deviations in the central wavelength of the FBG, caused by the tuning system.

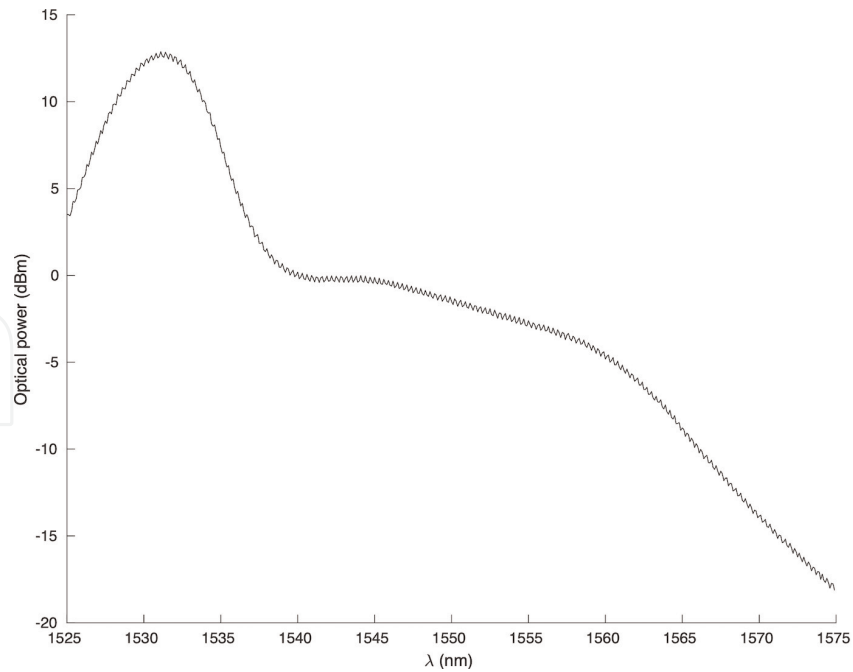


**Figure 4.** Optical spectrum of the ASE measured at the amplifier output for an optical pumping power value of 88 mW.

source with high spectral bandwidth. The input optical signal is amplified and introduced into the Bragg grating through an optical circulator. The signal reflected by the FBG is then conveyed by the circulator to an optical spectrum analyzer (ANRITSU model MS9601A). The Bragg grating is tuned by a motorized system developed for this purpose, which is described in ref. [25].

A commercial optical amplifier (Photonics model BT 13) with a pumping laser at 980 nm and an optical saturation power of 13 dBm was used.

**Figure 4** shows the ASE spectrum, measured with a resolution of 0.5 nm, where the dependence of the spectral amplitude with the wavelength is clearly visible. Therefore, all spectral measurements described in the following chapter are represented by subtracting the optical power of the source from the reflection spectrum, at each wavelength.

Bragg gratings are recorded on photosensitive single-mode fiber (Fibercore model PS1250/1500) with numerical aperture 0.13 and diameter 125  $\mu\text{m}$ . The etching method exposes the fiber to ultraviolet radiation through a constant period phase mask. The recording optical source is an Argon laser operating in continuous mode at 244 nm and with an average power of 150 mW. A more detailed description of the recording system can be found in [26, 27]. The apodization format of the network is approximately Gaussian because the laser used has an optical beam with a Gaussian profile.

## 4. Experimental results and discussion

### 4.1 Mechanical tuning

The tuning test, based on the scheme in **Figure 1**, is applied to a Bragg network with 1.5 cm long, half-height bandwidth 0.1 nm, center wavelength at 1556.94 nm, and rejection range of 10 dB. The length of the fiber containing the FBG is 18 cm, corresponding to the initial distance between the clamping presses.

According to studies carried out by several authors [18, 19], the maximum relative elongation that can be exerted on a silica optical fiber is 1%. To preserve the elasticity characteristics of the fiber, a more conservative value, around 0.5%, is considered the maximum limit. Regarding the fiber length used, it corresponds approximately to 0.9 mm. In the computerized tuning process, described in [25], this limit is considered to prevent the optical fiber from breaking.

**Figure 5** shows the reflection spectrum of the stretched Bragg grating. The maximum deviation from the central wavelength is 4.9 nm and corresponds to an offset of 0.98 mm. According to **Eq. (3)**, the relative elongation was 0.4%, remaining within the preestablished limit.

**Figure 6** shows the evolution of the bandwidth at 1, 3, and 10 dB, during the stretching process of the Bragg grating. Specifically, the bandwidth at 1 dB exhibits a variation within the range  $\pm 0.01$  nm, for the bandwidth of 3 dB there is an increase of 0.01 nm, and at 10 dB there is an increase of 0.05 nm in the bandwidth. Changes in maximum reflectivity are less than 1.1 dB.

The relationship between the variation of the central wavelength and the relative elongation is shown in **Figure 7**. The deviation from the central wavelength grows linearly as a function of relative elongation, at a rate of 0.85 pm/ $\mu\epsilon$  and with a correlation coefficient of 0.9951. The expected value for the growth rate, using expression (3), would be 1.2 pm/ $\mu\epsilon$ .

To verify whether this discrepancy is caused by imperfections in the motorized system, the influence of positioning errors on central wavelength tuning is calculated:

$$|d(\Delta\lambda_B)| \leq \left| \frac{\partial(\Delta\lambda_B)}{\partial(\Delta z)} \right| |d(\Delta z)| = \frac{0.78\lambda_B}{L} |d(\Delta z)|, \quad (10)$$

where  $|d(\Delta z)|$  is the tuning system accuracy (15  $\mu\text{m}$ ),  $L$  is the fiber length (18 cm) and  $\lambda_B$  is the Bragg wavelength of the Bragg grating at rest (1556.94 nm). With these

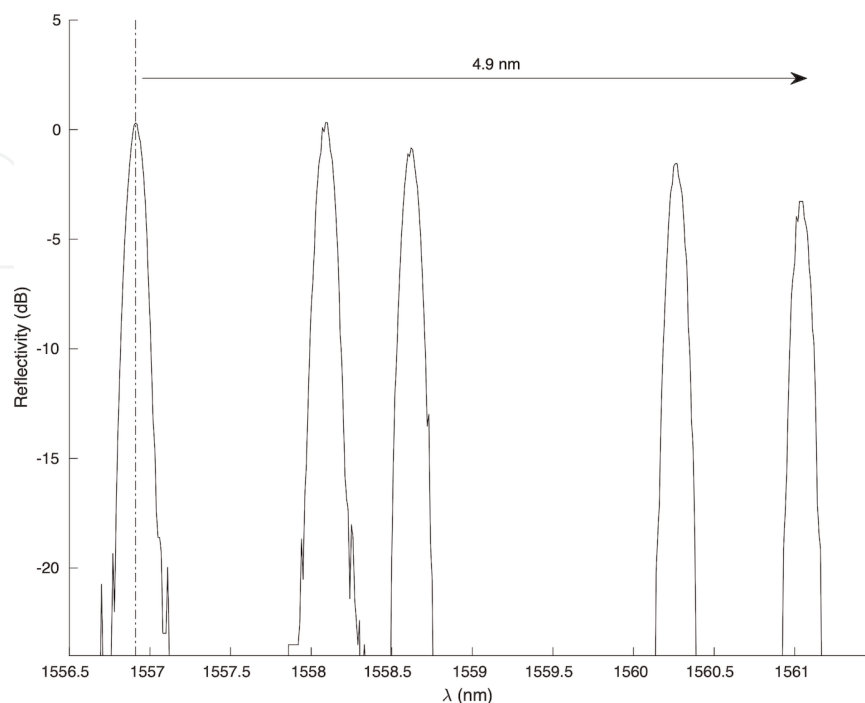


**Figure 5.**  
 Reflection profile of a Bragg grating under the effect of mechanical strain.

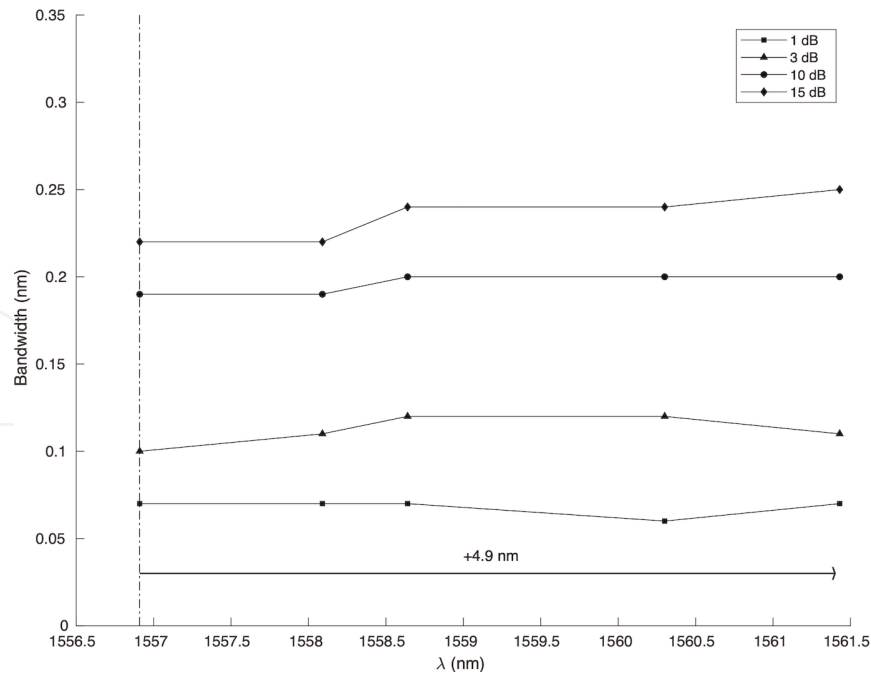


**Figure 6.**  
Bandwidth evolution over the entire tuning range.

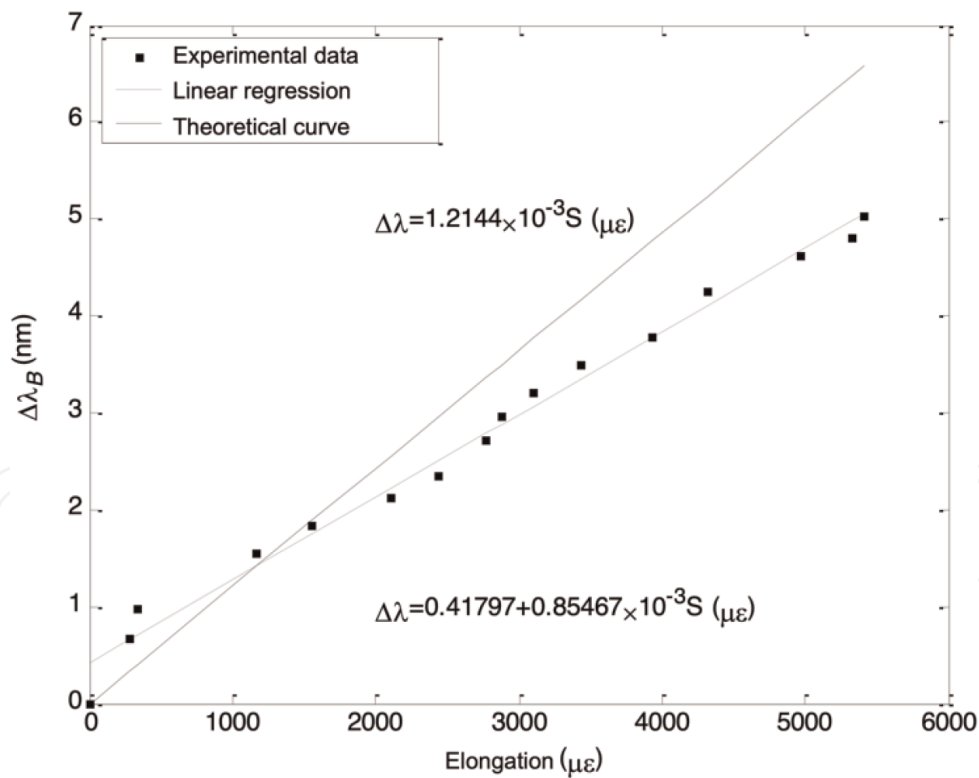


**Figure 7.**  
Bragg wavelength variation as a function of relative elongation.

values, the variation of the tuning value  $|d(\Delta\lambda_B)|$  is always less than or equal to 101 pm. If the error  $|d(\Delta\lambda_B)|$  is included in the set of measurements performed for the central wavelength, the resulting growth rate is in the range  $[0.84228, 0.85467]$  pm/ $\mu\epsilon$ . Therefore, imperfections in the motorized system are not the main cause of the differences.



A second tuning test had the scheme described in Section 2.2 as its working principle. In the first stage, the fiber is not embedded in an elastic material but fixed directly to the surface of a flexible sheet. The blade used is 15.2 cm long, 2 cm wide, and 1.5 mm thick, and is made of acrylic. A “v” shaped groove is created along the blade, 9 mm deep, to accommodate the fiber, so that it does not suffer transverse deviations. Consequently,  $d = 6$  mm (see Eq. (7)). The assembly is then glued to increase its strength and to properly fix the FBG inside the groove. Finally, the support is placed between the moving and fixed blocks of the tuning system to start the tests.

It was said earlier that the fiber can be stretched up to 1% without suffering irreversible damage. In compression mode, this value can reach 23% [19], which allows much larger tuning ranges than in elongation. Substituting Eq. (7) in (6), the resulting equation allows calculating a priori the maximum displacement allowed without damaging the fiber. Using more conservative values of 0.5% for compression and 11% for relative elongation, the calculated limits are, respectively, 9.96 mm and 14.13 cm.

The Bragg grating used is 2 cm long, it has a 3 dB bandwidth equal to 0.48 nm and a central wavelength of 1550.4 nm. During the tests, the amplitude of the reflection spectrum was recorded by an optical spectral analyzer, at several tuning points, as shown in Figure 8.

The results show that the variation achieved in the central wavelength, using compression, and stretching forces reaches practically 19 nm. It is visible in Figure 8 that there is a gap in the initial phase of the stretching tuning process. This failure occurred simply because the spectral measurement process was started with the Bragg grating already under the effect of a sufficiently strong mechanical stress that the central wavelength was shifted from its initial value of 1550.4 nm.

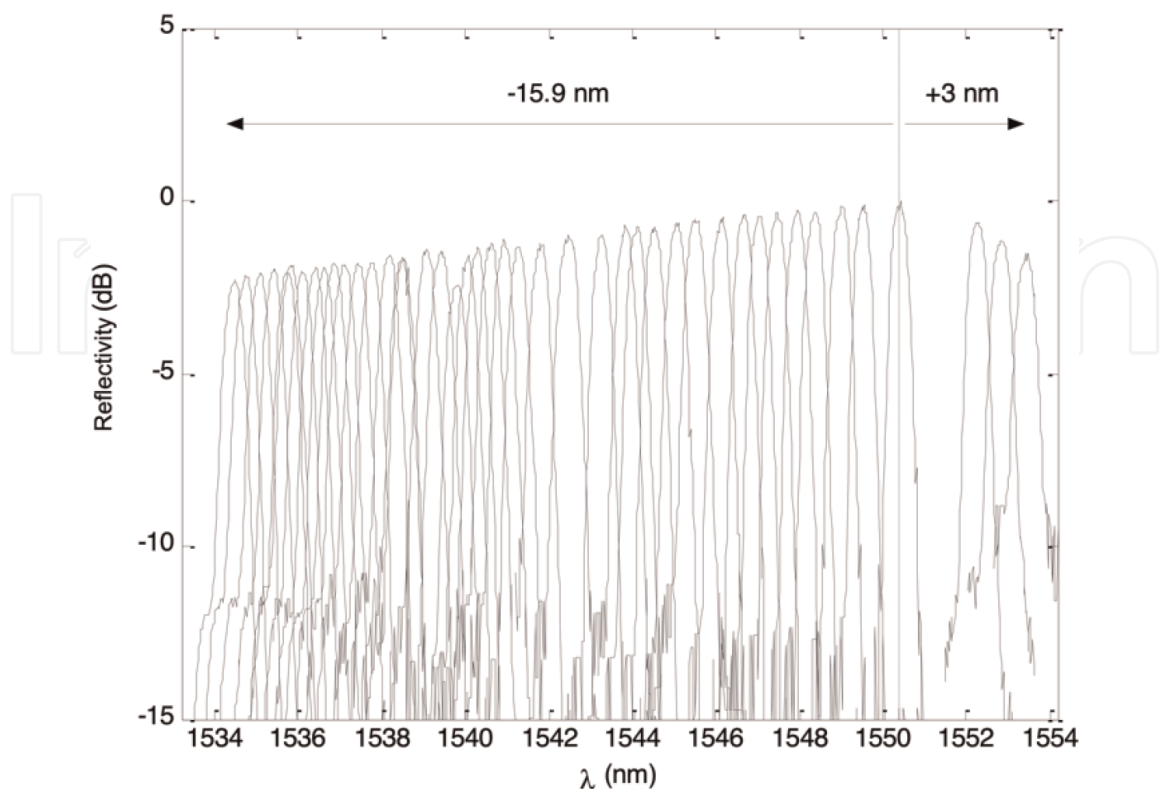


**Figure 8.**  
*Tuning the central wavelength of the Bragg grating at 18.9 nm.*

It is possible to obtain better results, especially in compression mode, as the mobile platform moved only 6.8 cm to obtain a variation of  $-15.9$  nm. However, the mechanical characteristics of the acrylic sheet did not allow to compress the fiber further. On the other hand, the 3 nm spectral variation in stretching mode was achieved by moving the system 4.3 mm and could theoretically reach 4.2 nm with a displacement equal to 9.96 mm.

**Figure 9** shows the relationship between tuning range  $\Delta\lambda$  and normalized length  $\Delta z/L$ .

The results show a good agreement between the theoretical curve, calculated by **Eq. (8)**, and most of the measurements performed.

The main differences are located at the ends of the graph, which correspond to situations of greater mechanical stress. They are somehow correlated with the progressive decrease in the maximum reflectivity amplitude, visible in **Figure 8**. These changes can be caused by undetected problems in the tuning system. In particular, the glue used can lose its fixing qualities when subjected to large deformations, resulting in bends on the fiber [18].

The evolution of the bandwidth at 1, 3, and 10 dB is represented in **Figure 10**. Starting from the initial position, the axial mechanical forces applied on the FBG do not cause great changes in the width at 3 dB, which oscillates between  $-0.1$  and  $0.04$  nm. The bandwidth at 1 dB also remains practically constant, with a maximum deviation of 12.5% from the initial value. However, the bandwidth at 10 dB undergoes a gradual increase that reaches  $0.4$  nm in compression and  $0.56$  nm in stretching, in addition to showing an irregular behavior.

The increase in bandwidth at 10 dB is clearly visible in **Figure 11**, where the reflection spectrum is not symmetrical, especially when the FBG is subjected to strong

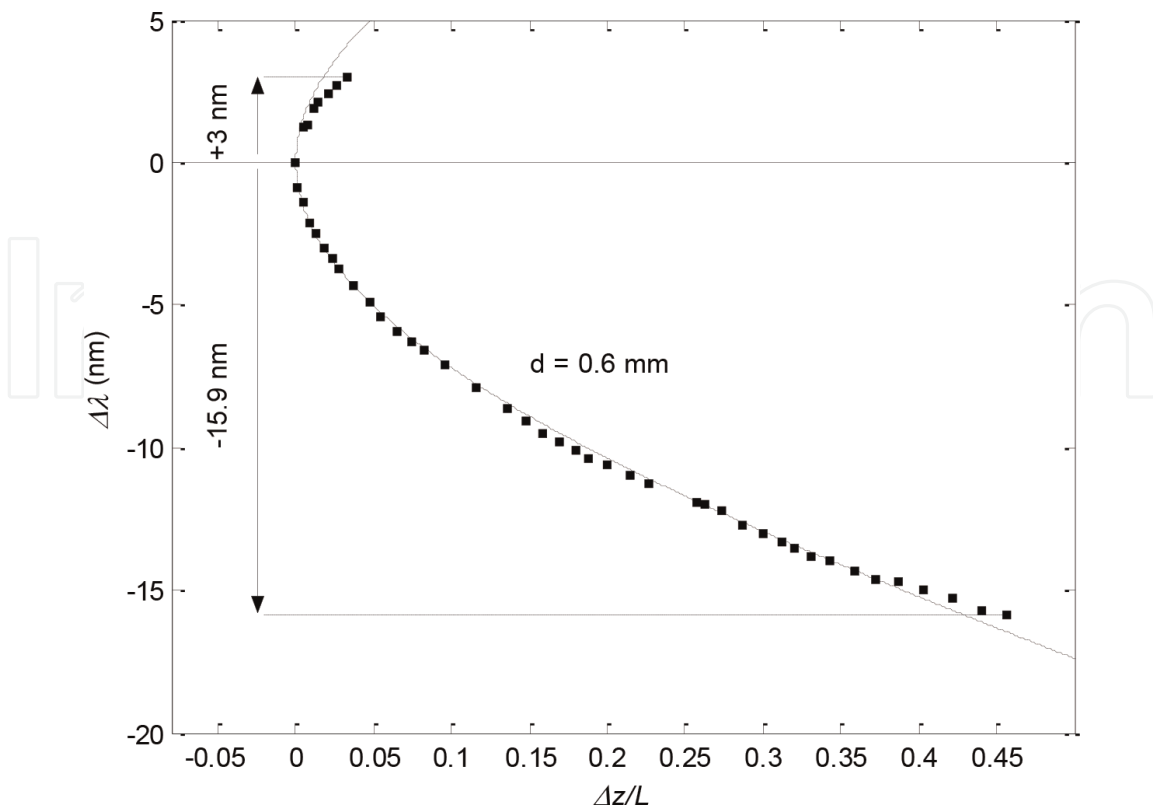


**Figure 9.** Wavelength variation as a function of normalized horizontal displacement. (Dashed line: theoretical value, points: measured values).

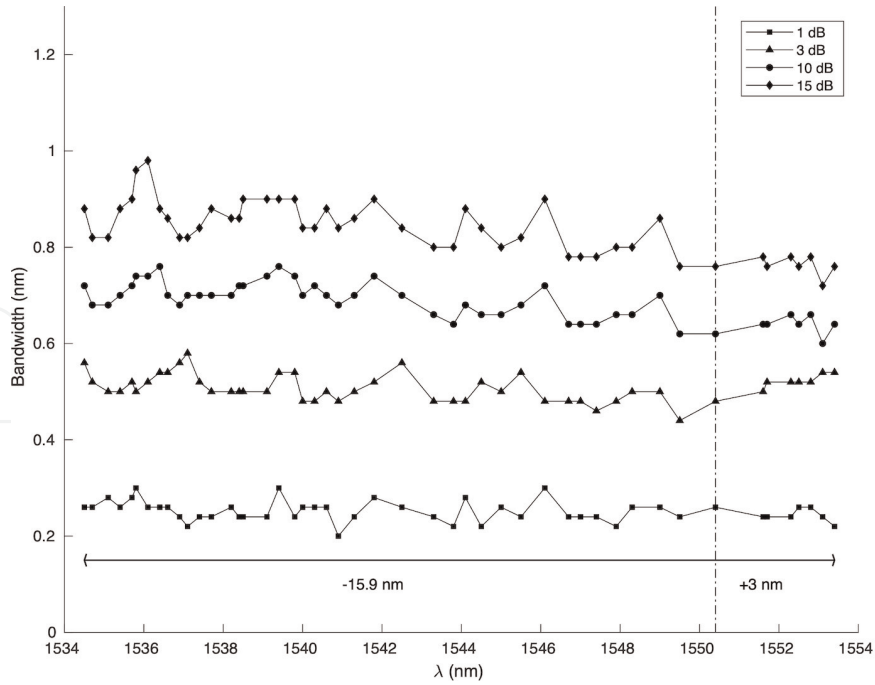


**Figure 10.**  
 Bandwidth evolution over the entire tuning range.

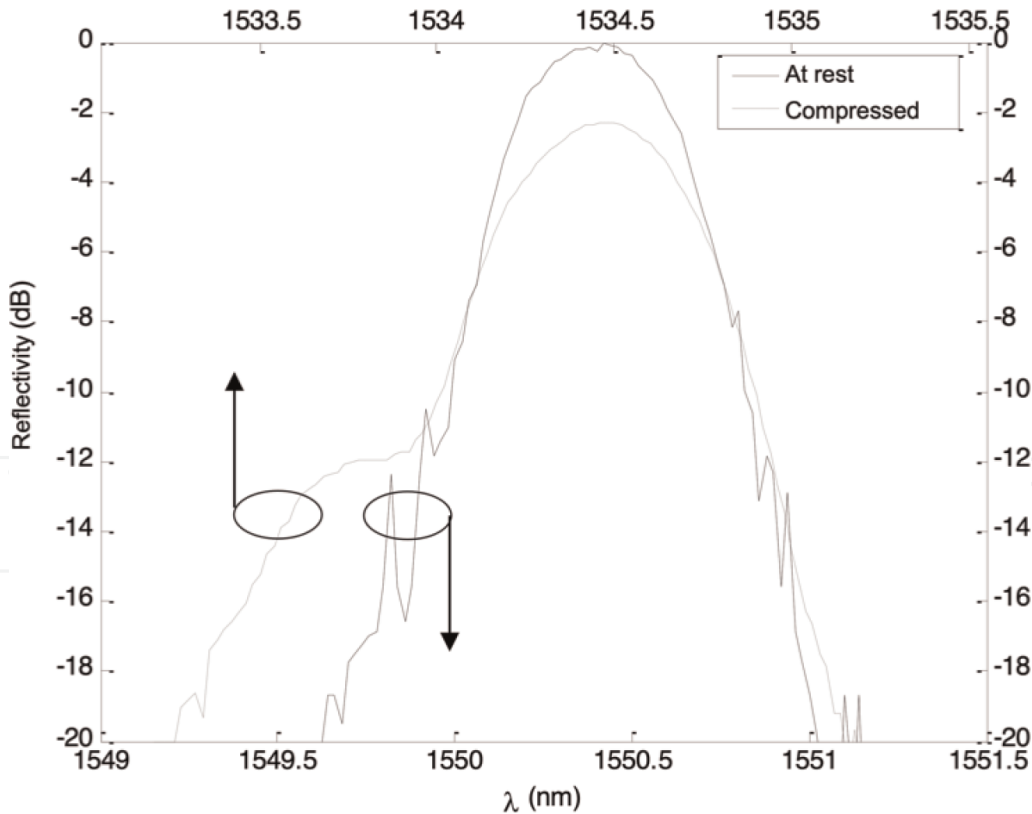


**Figure 11.**  
 Spectral response of a Bragg grating at rest (solid line) and under compression (dashed line).

compressions. Under these conditions, the pressure exerted along the grating is not uniform, which causes a variation in the grating period  $\Lambda$  and consequently a chirped spectrum. Consequently, the coupling between the propagation modes within the

FBG is no longer tuned to just one wavelength, thus decreasing the maximum reflectivity amplitude, and increasing the width at the base of the reflection spectrum.

On the other hand, the irregularities observed are largely due to the noise level being very close to 10 dB, causing sudden and profound variations in the reflectivity value.

According to Eq. (7), the tension exerted on a Bragg grating, fixed at a distance  $d$  from the flexible blade, makes it possible to increase the tuning range without changing the length  $L$ . Theoretically, it is possible to move the reflection spectrum by 50 nm, even for small  $\Delta z$  deviations [7].

Another tuning test was performed with a Bragg grating with a reflectivity peak at 1546.3 nm, 3 dB spectral width equal to 0.46 nm and length 1.5 cm. The FBG was inserted into silicone, 6 mm away from the surface of a flexible acrylic base 16 cm long.

Figure 12 shows the relationship between the tuning range and the normalized travel distance. The measured tuning points do not follow the theoretical curve for  $d = 6$  mm. The main cause for this deviation is a cause of the elastic properties of silicone. The curvature of the acrylic base is not followed by the silicone surface where the Bragg grating is inserted. Thus, the resulting tuning is much smaller than expected.

This problem is accompanied by a progressive decrease in the maximum reflectivity amplitude and in the broadening of the reflection spectrum, visible in Figure 13. The FBG reflectivity decreases by 3 dB over approximately 8 nm of tuning. The spectral widths at 1, 3, and 10 dB increase by 0.07, 0.29, and 1.33 nm, respectively.

#### 4.2 Temperature tuning

To verify the dependence of the central reflection wavelength of the Bragg grating on temperature, the reflectivity spectrum of a grating centered initially at 1548.11 nm,

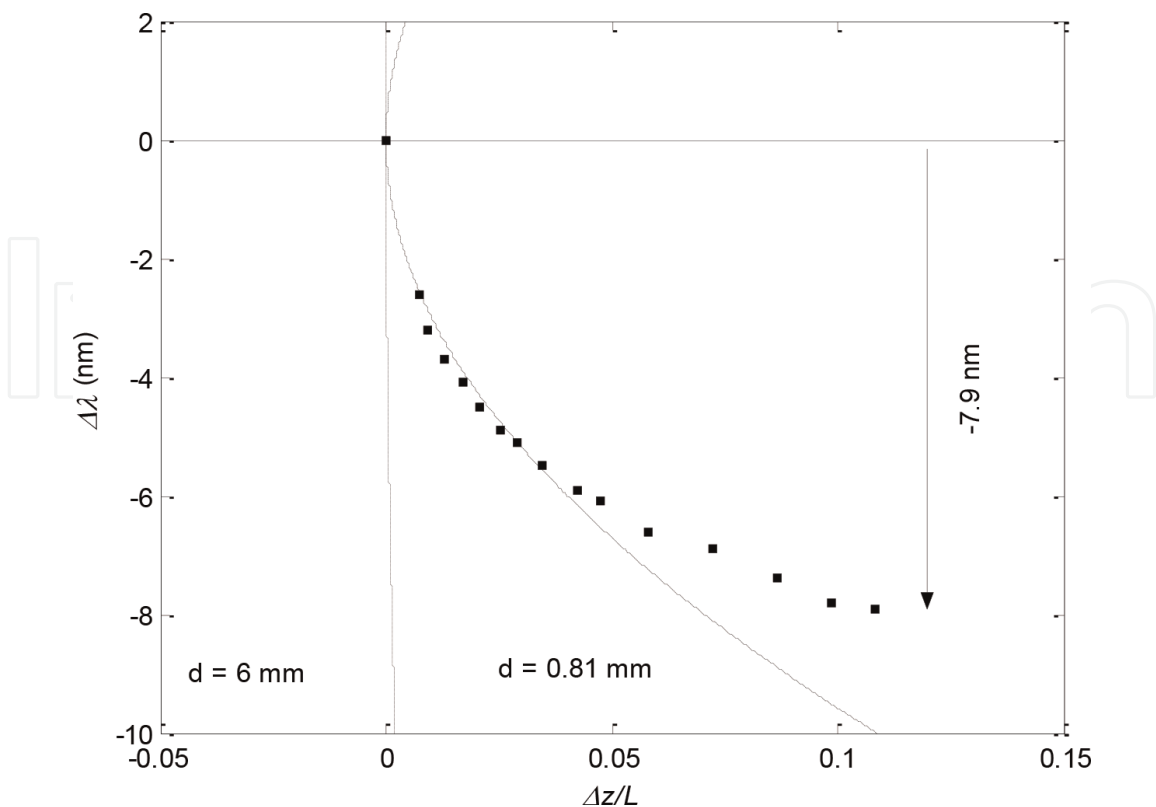
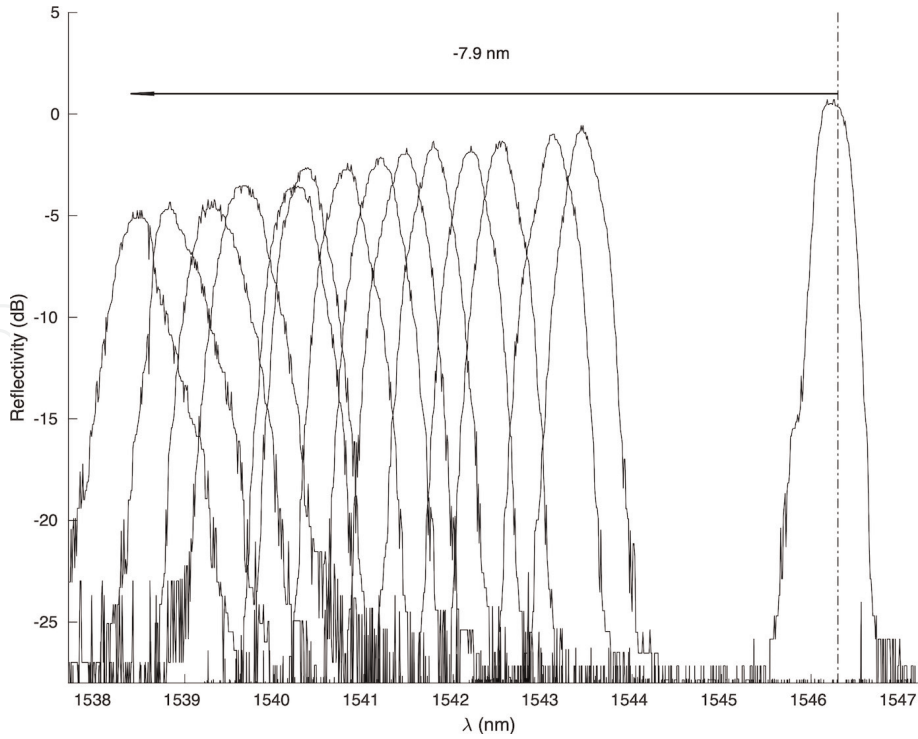
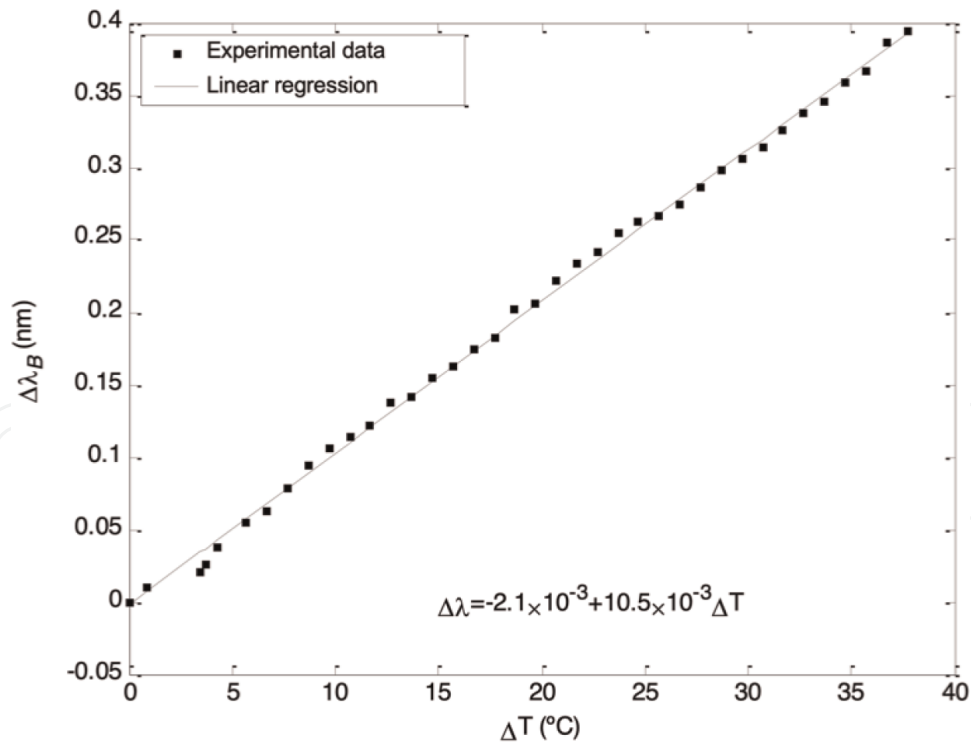


Figure 12. Wavelength variation as a function of normalized horizontal displacement. (Dashed line: theoretical values, points: measured values).



**Figure 13.**  
 Bragg grating tuning at 7.9 nm.



**Figure 14.**  
 Bragg wavelength variation as a function of FBG temperature (dashed line: theoretical value, points: measured values).

at a temperature of 14.3°C, was measured. The tuning method is based on the procedure described in Section 2.3. **Figure 14** shows the tuning results achieved at the expense of temperature variation in the Bragg grating. The tuning range accomplished

was 0.4 nm, for a temperature variation of 40°C, and follows a linear relation between temperature and central wavelength variations.

## 5. Conclusion

In this chapter, two tuning processes for fiber Bragg gratings were presented: By mechanical stress on the fiber grating, or by changing its temperature.

In the first method, the optical fiber is more resistant to compression than to extension. The tuning range of the Bragg grating reflects this behavior, and therefore the Bragg grating must be produced with an initial central wavelength close to the upper tuning limit to increase the effective tuning wavelength span.

In the bending compression method, the material supporting the Bragg grating must be elastic enough to allow it to bend but must have the necessary rigidity to follow the curvature of the acrylic base. Therefore, silicone is not a suitable option for this tuning process, and other material with appropriate properties should be investigated.

The temperature tuning process achieved a poor tuning range (0.4 nm) compared to the mechanical tuning processes (19 nm), and it requires a permanent current source so that the Peltier cells can maintain the fiber grating temperature constant. The mechanical tuning system does not require the use of bulky and expensive current sources and maintains the desired tuning even if the electrical system is turned off. This is an additional advantage, which partially reduces electrical energy consumption. Furthermore, the spectral bandwidth (1, 3, and 10 dB) is maintained over a broad tuning range, but extreme bending or stretching of the fiber may chirp the Bragg grating and increase its spectral bandwidth.


### Author details

Rogério Dionísio

Polytechnic Institute of Castelo Branco, DiSAC – Digital Services, Applications and Content, Castelo Branco, Portugal

\*Address all correspondence to: [rdionisio@ipcb.pt](mailto:rdionisio@ipcb.pt)

### IntechOpen

© 2022 The Author(s). Licensee IntechOpen. This chapter is distributed under the terms of the Creative Commons Attribution License (<http://creativecommons.org/licenses/by/3.0>), which permits unrestricted use, distribution, and reproduction in any medium, provided the original work is properly cited. 

## References

- [1] Hill KO, Fujii Y, Johnson DC, Kawasaki BS. Photosensitivity in optical fiber waveguides: Application to reflection filter fabrication. *Applied Physics Letters*. 1978;**32**(10):647-649
- [2] Meltz G, Morey WW, Glenn WH. Formation of Bragg gratings in optical fibers by a transverse holographic method. *Optics Letters*. 1989;**14**(15):823-825
- [3] Hill KO, Meltz G. Fiber Bragg grating technology fundamentals and overview. *Journal of Lightwave Technology*. 1997;**15**(8):1263-1276
- [4] Russell PS, Archambault JL, Reekie L. Fibre gratings. *Physics World*. 1993;**6**(10):41-46
- [5] Li C, Tang J, Cheng C, Cai L, Yang M. FBG arrays for quasi-distributed sensing: A review. *Photonic Sensors*. 2021;**11**(1): 91-108
- [6] Ahlawat D, Arora P, Kumar S. Performance evaluation of proposed WDM optical link using EDFA and FBG combination. *Journal of Optical Communications*. 2019;**40**(2):101-107
- [7] Giles CR. Lightwave applications of fiber Bragg gratings. *Journal of Lightwave Technology*. 1997;**15**(8):1391-1404
- [8] Radzi NM, Latif AA, Ismail MF, Liew JY, Awang NA, Lee HK, et al. Tunable spacing dual-wavelength Q-switched fiber laser based on tunable FBG device. *Photonics*. 2021;**8**(12):524 MDPI
- [9] Singh H, Sheetal A. Suitability of FBG for gain flatness of  $64 \times 10$  Gbps DWDM system using hybrid (EDFA + YDFA) optical amplifier in C + L band up to 50 GHz (0.4 nm) channel spacing. *Journal of Optical Communications*. 2019. DOI: 10.1515/joc-2019-0134
- [10] Othonos A, Kalli K, Kohnke GE. Fiber Bragg gratings: Fundamentals and applications in telecommunications and sensing. *Physics Today*. 2000;**53**(5):61
- [11] Hunter DB, Minasian RA. Programmable high-speed optical code recognition using fibre Bragg grating arrays. *Electronics Letters*. 1999;**35**(5): 412
- [12] Cheng HC, Wijanto E, Lien TC, Lai PH, Tseng SP. Multiple access techniques for bipolar optical code division in wireless optical communications. *IEEE Access*. 2020;**8**: 83511-83523
- [13] Boukricha S, Ghomid K, Mekaoui S, Ar-Reyouchi E, Bourouina H, Yahiaoui R. SAC-OCDMA system performance using narrowband Bragg filter encoders and decoders. *SN Applied Sciences*. 2020;**2**(6):1-9
- [14] McGeehan JE, Hauer MC, Willner AE. Optical header recognition using fiber Bragg grating correlators. *IEEE LEOS Newsletter*. 2002;**16**(4):29-32
- [15] Agrawal GP. *Applications of Nonlinear Fiber Optics*. London Elsevier: Ap, Academic Press; 2021
- [16] Othonos A, Kalli K. *Fiber Bragg gratings: Fundamentals and Applications in Telecommunications and Sensing*. Boston, Mass.: Artech House; 1999
- [17] Ibsen M, Set SY, Goh GS, Kikuchi K. Broadband continuously tunable all-fiber DFB lasers. *IEEE Photonics Technology Letters*. 2002;**14**(1):21-23

- [18] Iocco A, Limberger HG, Salathe RP, Overall LA, Chisholm KE, Williams JAR, et al. Bragg grating fast tunable filter for wavelength division multiplexing. *Journal of Lightwave Technology*. 1999; **17**(7):1217-1221
- [19] Goh CS, Mokhtar MR, Butler SA, Set SY, Kikuchi K, Ibsen M. Wavelength tuning of fiber Bragg gratings over 90 nm using a simple tuning package. *IEEE Photonics Technology Letters*. 2003; **15**(4):557-559
- [20] Mokhtar MR, Goh CS, Butler SA, Set SY, Kikuchi K, Richardson DJ, et al. Fibre Bragg grating compression-tuned over 110 nm. *Electronics Letters*. 2003; **39**(6):509
- [21] Set SY, Dabarsyah B, Goh CS, Katoh K, Takushima Y, Kikuchi K, et al. A widely tunable fiber Bragg grating with a wavelength tunability over 40 nm. In *Optical Fiber Communication Conference 2001 Mar 17* (p. MC4). Optical Society of America
- [22] Mokhtar MR, Ibsen M, Teh PC, Richardson DJ. Simple dynamically reconfigurable OCDMA encoder/decoder based on a uniform fiber Bragg grating. In *Optical Fiber Communication Conference 2002 Mar 17* (p. ThGG54). Optica Publishing Group
- [23] Ohn MM, Alavie AT, Maaskant R, Xu MG, Bilodeau F, Hill KO. Dispersion variable fibre Bragg grating using a piezoelectric stack. *Electronics Letters*. 1996; **32**(21):2000
- [24] Dabarsyah B, Goh CS, Khijwania SK, Set SY, Katoh K, Kikuchi K. Adjustable dispersion-compensation devices with wavelength tunability based on enhanced thermal chirping of fiber Bragg gratings. *IEEE Photonics Technology Letters*. 2003; **15**(3): 416-418
- [25] Dionísio RP. Módulo de Posicionamento Micrométrico: Projecto, Construção e Caracterização. 1<sup>o</sup> Workshop de Investigação e Desenvolvimento em Engenharia Eletrotécnica e das Telecomunicações [Internet]. 2004 Feb 18 [cited 2022 Jun 27]. pp. 43-48. Available from: <http://hdl.handle.net/10400.11/8003>
- [26] de Brito André PS. Componentes optoelectrónicos para redes fotónicas de alto débito (Doctoral dissertation, Universidade de Aveiro (Portugal))
- [27] Nogueira RN. Redes de Bragg em fibra óptica (Doctoral dissertation, Universidade de Aveiro (Portugal))